

# DRAINAGE EROSION AND CONCAVE LANDFORM OF TIJUCA GNEISSIC MASSIF, STATE OF RIO DE JANEIRO, BRAZIL, WITH THE HELP OF SUMMIT LEVEL AND BASE LEVEL TECHNIQUE BASED ON ASTER GDEM

Akihisa MOTOKI <sup>1</sup>, Susanna Eleonora SICHEL <sup>2</sup>; Samuel da SILVA <sup>2</sup>, Kenji Freire MOTOKI <sup>2</sup>; Aurélio Kasakewitch RIBEIRO <sup>1</sup>

(1) Departamento de Mineralogia e Petrologia Ígnea, Universidade do Estado do Rio de Janeiro (DMPI/UERJ). Rua São Francisco Xavier 524, Sala A-4023, Maracanã, Rio de Janeiro, CEP 20550-900, RJ. E-mail: motokiakihisa@gmail.com, aureliokr@uol.com.br.

(2) Departamento de Geologia, Universidade Federal Fluminense (DG/UFF). Av. General Milton Tavares de Souza s/n, 4º andar, Gragoatá, Niterói, CEP. 24210-340, RJ. E-mail: susanna@id.uff.br, samueltec@gmail.com, kenji\_dl@hotmail.com.

Introduction  
Research methods  
Tijuca gneissic massif  
Summit level maps  
Base level maps  
Relief amount maps and MCI  
Altitude distribution histogram  
Three-dimensional concavity index  
Discussion  
Conclusion  
Acknowledgement  
Reference

**RESUMO** - Motoki, A. Sichel, S.E., Silva, S., Motoki, K.F. *Erosão por drenagens e morfologia côncava do maciço gnáissico da Tijuca, RJ, com o auxílio das técnicas de seppômen e sekkokumen com base no ASTER GDEM.* Este trabalho apresenta o estado de erosão por drenagens e a concavidade tridimensional do maciço gnáissico de Tijuca, Município do Rio de Janeiro, por meio das análises geomorfológicas com base no ASTER GDEM. O maciço tem uma extensão de 15 x 10 km e altitude relativa de 1000 m e, é constituído principalmente por ortogneisse e paragneisse. Os mapas de seppômen mostram a ausência de escarpa marginal e a área limitada do platô virtual. O maciço é dividido em Floresta da Tijuca e Serra da Carioca pela zona de vale do Alto de Boa Vista, com largura maior do que 2 km. Os pequenos morros rochosos formam cinco alinhamentos paralelos com orientação de N60°E. Os mapas de sekkokumen apresentam as drenagens com largura maior do que 1 km orientando a N45°E, que é diferente de orientação dos morros. As drenagens estreitas e curtas na zona mais alta da serra constituem um sistema radial. As áreas da Floresta da Tijuca, Serra da Carioca e Pedra da Gávea possuem alto kifukuryo, com o risco de deslizamento de grande escala. Essas são caracterizadas por exposições subverticais de gnaisse. O histograma de distribuição altimétrica mostra distribuição parecida à forma da Torre Eiffel, indicando a forma tridimensional côncava do maciço. Os índices de concavidade tridimensional (TCI) e de macro concavidade (MCI) são, respectivamente, 0.54 e -0.5 que são significativamente maiores do que os maciços de rochas alcalinas félsicas. A forma côncava do maciço Tijuca é atribuída à vulnerabilidade erosiva do gnaisse, devido à fraqueza mecânica, textura de gnaisse e baixos efeitos da passividade intempérica.

**Palavras-chave:** Maciço Tijuca, seppômen, sekkokumen, TCI, MCI, GDEM.

**ABSTRACT** – This paper presents the state of drainage erosion and three-dimensional concavity of Tijuca gneissic massif, Municipal District of Rio de Janeiro, Brazil, by means of geomorphologic analyses based on the ASTER GDEM. The massif has an extension of 15 x 10 km and relative height of 1000 m. The summit level maps show absence of marginal scarp and limited area of virtual plateau. The massif is divided into Tijuca Forest and Carioca Range by Alto da Boa Vista valley zone, which is wider than 2 km. Small rocky hills form five parallel chains with N60°E orientation. The base level maps present the drainages wider than 1 km striking to N45°E, which is different from the hill orientation. The narrow and short drainages at the highest range zone constitute a radial system. The areas of Tijuca Forest Range, Carioca Range, and Gávea Rock have high relief amount with the risk of large-scale landslide. They are characterised by subvertical gneiss exposures. The altitude distribution histogram shows an Eiffel Tower-like pattern, indicating concave three-dimensional landform of the massif. The volume-normalised three-dimensional concavity index (TCI) and macro concavity index (MCI) are, respectively, 0.54 and -0.5, which are significantly larger than those of the felsic alkaline massifs. The concave landform of Tijuca massif is attributed to erosive vulnerability of the gneiss because of low mechanical strength, gneissic texture, and low weathering passivity effects.

**Keyword:** Tijuca massif, summit level, base level, TCI, MCI, GDEM.

## INTRODUCTION

The Tijuca massif occurs in the municipal district of Rio de Janeiro, southeastern Brazil. This massif has 15 x 10 km of extension and 1000 m of relative height and its central area is situated at 22°58'S and 43°15'W (Figure 1).

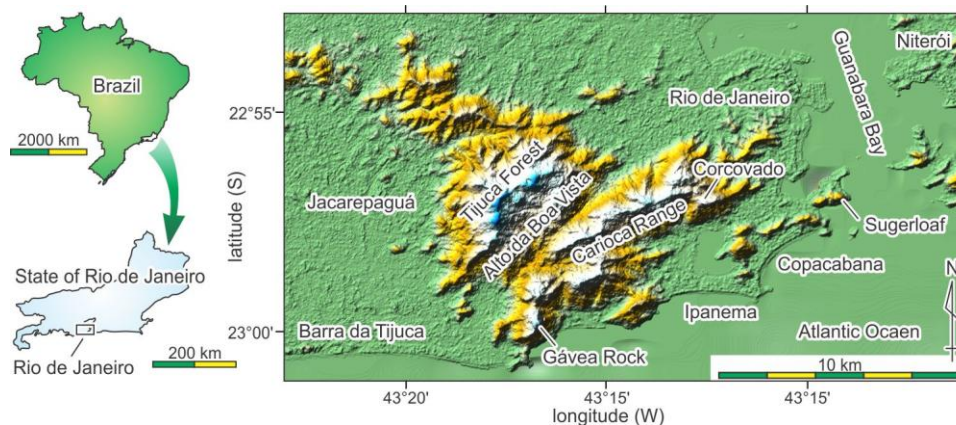


**Figure 1.** Relief map of Tijuca massif, Municipal District of Rio de Janeiro, Brazil, based on ASTER GDEM.

This massif is made up mainly of late Pan-African orthogneiss and paragneiss (e.g. Heilbron et al., 2000; Heilbron & Machado, 2003; Kühn et al., 2004). The metamorphic basement is cut by dyke-like post-tectonic intrusions of Andorinha Granite (Valeriano et al., 2011) and silicified fault breccia zones (Motoki et al., 2011; 2012a). They are intruded by Early Cretaceous mafic dykes (Guedes et al., 2005; Motoki et al., 2009).

This area has frequent occurrences of cloudbursts and the consequent debris-flow type landslides. For the mitigation of disasters, many efforts have been paid in geotechnics, engineering, and rock weathering (e.g. Fernandes et al., 2004; Coelho Netto et al.,

2007; 2009; Marques et al., 2010; Ramli et al., 2010). In order to clarify landslide mechanism and hazard map confection, regional morphologic and geologic studies are important, especially of Tijuca massif.

The authors have performed geomorphologic analyses of Tijuca gneissic massif based on satellite-derived topographic data of ASTER GDEM, with the help of summit level and base level techniques, altitude distribution histogram, volume-normalised three-dimensional concave index (TCI), and macro concavity index (MCI). This article presents the results and discusses the origin of the present-day landscapes characterized by large rock exposures.

## RESEARCH METHODS

The authors have adopted the following highlighted methods: 1) Summit level map; 2) Base level map; 3) Relief amount map; 4) Altitude distribution histogram; 5) Volume-normalised three-dimensional concavity index (TCI); 6) Macro concavity index (MCI).

Summit level (*seppômen*) and base level (*sekkokumen*) maps are the virtual topographic maps which show respectively the palaeo morphology before vertical drainage erosion and the future morphology to be formed by lateral erosion. The former is constructed by highest points extracted from the original topographic map, such as peaks and crests (Motoki et al., 2008a), and the latter, by the lowest points, as valley bottoms (Motoki et al., 2014). Relief amount (*kifukuryo*) is constructed by the difference between the summit level and base level (Motoki et al., 2015a).

These maps are constructed from the satellite-derived digital elevation model of ASTER GDEM (Global Digital Elevation Map), which is released by ERSDAC (Earth Remote Sensing Analyses Center). The data are processed by the original software BAZ 1.0, Build 71, which elaborates simultaneously summit level, base level, and relief amount maps of grid intervals of 1920 m, 960 m, 480 m, 240 m, 120 m, and 60 m. The technical details of the map confection methods are shown in Motoki et al. (2008a; 2014a) and Aires et al. (2012). The calculated results are using kriging function with the help of Surfer™ ver. 8.0.

The macro concavity index (MCI) provides three-dimensional form of massive, if it is convex or concave. Calculation of this parameter needs summit level and relief amount data (Motoki et al., 2008a; 2012a; 2014; Motoki K.F. et al., 2014). The volume-

normalised three-dimensional concavity index (TCI) is a new parameter proposed by this article with similar objective of MCI. The massifs with positive TCI have concave three-dimensional landform of advanced erosion stage, and those with negative TCI, convex

form of young erosion stage. The details are written in the chapter of three-dimensional concavity index of this article. The diagram of TCI vs. MCI distinguishes erosive resistance degree of the base rock.

## TIJUCA GNEISSIC MASSIF

The Tijuca massif has an extension of 15 km (E-W) x 9.5 km (N-S), total an area of 85 km<sup>2</sup>, and a relative height of 1000 m. The massif stands up from the coastal plane on which the urban zone of Rio de Janeiro is situated. The highest point is Tijuca Peak (*Pico da Tijuca*, 1021 m of altitude) and the second one is Papagaio Beak (*Bico do Papagaio*), 989 m. The massif is divided into two areas by a deep linear valley zone with a strike of N45°E, called Alto de Boa Vista. The fieldworks have recognizes no notable fault and shear zone along this valley.

The north-western area is called Tijuca Forest Range (*Floresta da Tijuca*), where highest peaks take place. The south-eastern one is Carioca Range (*Serra da Carioca*), which is about 300 m lower than the Tijuca Forest. The both areas belong to Tijuca National Park.

The border of Tijuca massif is not so sharply delimited and has complex star-like dendritic shape. It is contrasted with the sharp rounded or elliptic border of the felsic alkaline

intrusive massifs of this region (Motoki et al., 2008a; 2014).

The main constituent rocks of Tijuca massif are paragneiss and orthogneiss with metamorphic ages of 590-565 Ma and 535-520 Ma (Machado et al. 1996). The Tijuca Forest Range and the adjacent areas are constituted mainly by migmatitic paragneiss. They are composed of biotite gneiss with minor occurrences of garnet biotite gneiss. The paragneiss have migmatitic texture with pegmatitic neosome (Figure 2A). The proportion of the neosome increases from southeast, 5% at Alto da Boa Vista, to northwest, more than 50% on the western slope of the massif to Jacarepaguá urban zone (Figure 1). The gneissic rocks tend to form large walls of rock exposure (Figure 2B), such as Tijuca Peak and Conde Rock (*Pedra do Conde*, 819 m). Different from the previous idea (e.g. Helmbold et al., 1965), no horizontal granitic cap body is found on the top of these peaks.



**Figure 2.** Rocks of Tijuca massif: A) Migmatitic biotite gneiss at Cascatinha Fall; B) Tijuca Peak (*Pico da Tijuca*) and Conde Rock (*Pedra do Conde*) constituted by paragneiss; C) Papagaio Beak (*Bico do Papagaio*) made up of granite; D) Gávea Rock (*Pedra da Gávea*) composed of orthogneiss and granite. Gn - gneiss; Gr - granite; Pg - pegmatitic neosome.

At Alto da Tijuca Highland, in the western part of Alto da Boa Vista, there is an intrusive body of quartz diorite with an extension of 1.5 km. This rock has relevant black macroscopic colour and it was extracted for ornamental uses with commercial name of Tijuca Black (*Granito Preto Tijuca*, Motoki et al., 2006).

Many dyke-like post-tectonic monzogranite (3b) are found in Tijuca Forest Range with U-Pb ages of ca. 480 Ma (Valeriano et al., 2011), called Andorinha Granite (Penha et al., 1979) or Favela Granite (Pires et al., 1982). The granitic tykes are from 1 m to 100 m wide and have NW-SE orientation. They cut the metamorphic basement and Alto da Tijuca Quartz Diorite. Some highest peaks, as Papagaio Beak (*Bico do Papagaio*), Cocanha Hill (*Morro da Cocanha*, 982 m), and Taquara Hill (*Morro da Taquara*, 814 m), are constituted by this granite (Figure 2C). They tend to be more frequent from southeast to northwest.

Carioca Range and the adjacent areas are constituted mainly by non-migmatitic granitic orthogneiss. A part of them has augen texture and some outcrops exhibit garnet porphyroblasts, the rock called kinzigite. Leucocratic garnet quartz gneiss (leptinite) also is found. Several international sightseeing spots of Rio de Janeiro, such as Sugarloaf Mountain (*Morro de Pão de Açúcar*), Corcovado (*Morro do Corcovado*), Arpoador (*Ponta de Arpoador*),

and Gávea Rock (*Pedra da Gávea*; Figure 2D) expose augen gneiss. The other areas crop out orthogneiss with less developed or without augen texture. The Andorinha post-tectonic granitic dykes are little expressive in this area.

Top of Gávea Rock (*Pedra da Gávea*; 844 m) and that of Bonita Rock (*Pedra Bonita*; 693 m) exhibit bottom zone of a granitic pluton with horizontal intrusive contact with the basement gneiss. The granite of Gávea Rock has abundant alkaline feldspar phenocryst of 5 to 10 cm in length. These bodies are considered to be eastern extension of funnel-shaped granitic intrusion of Pedra Branca. The U-Pb ages of Pedra Branca Granite are little older the Andorinha Granite, ca. 513 Ma (Valeriano et al., 2011).

The above-mentioned bodies are cut by silicified tectonic breccia of the last stage of the Pan-African continental collision event (Motoki et al., 2011; 2012a). The fault breccia zones are scattered widely in State of Rio de Janeiro, including urban zone of Rio de Janeiro,

All of them are intruded by early Cretaceous tholeiitic dykes of Paraná Province (Stewart et al., 1996; Guedes et al., 2005; Motoki et al., 2009). There are felsic alkaline intrusions of the Cretaceous to early Cenozoic associated with vent-filling subvolcanic welded pyroclastic rocks (e.g. Motoki et al., 2007a; b; c; 2008b; c; 2012b; Sichel et al., 2008; Geraldés et al., 2013). However, no alkaline bodies are found within Tijuca massif.

## SUMMIT LEVEL MAPS

In a massif of young erosive stage, summit level map reproduces original elevated peneplane from the fragmented areas of remand surface. However, in a massif of advanced stage, summit level map cannot reproduce the original peneplane and shows development stage of peaks and crests. It is useful to study erosive resistance of the base rock.

The summit level map for Tijuca massif of 960 m of grid interval show smooth surface, distinguishing Tijuca Forest Range (TJF, Figure 3A) and the south-western one, Carioca Range (CRR). They have respective strikes of N45°E to N60°E. The virtual plateau occurs along Alto da Boa Vista (ABV). It has about 600 m of

altitude and 4 km (NE-SW) x 2 km (NW-SE) of extension. The massif border is characterised by moderately dendritic shape. No morphologic characteristics of vertical fault displacement are observed.

This map shows the valleys wider than 2 km. There are five observable valleys and four of them have NE-SW strike. The largest one is Alto da Boa Vista valley zone along the drainages D1 and D2, with strike of N45°E and total length of 10 km. Some of minor drainages, such as D3, D8, and D21, cut across the virtual ranges and plateau, indicating deep and narrow valleys formed by strong vertical erosion.

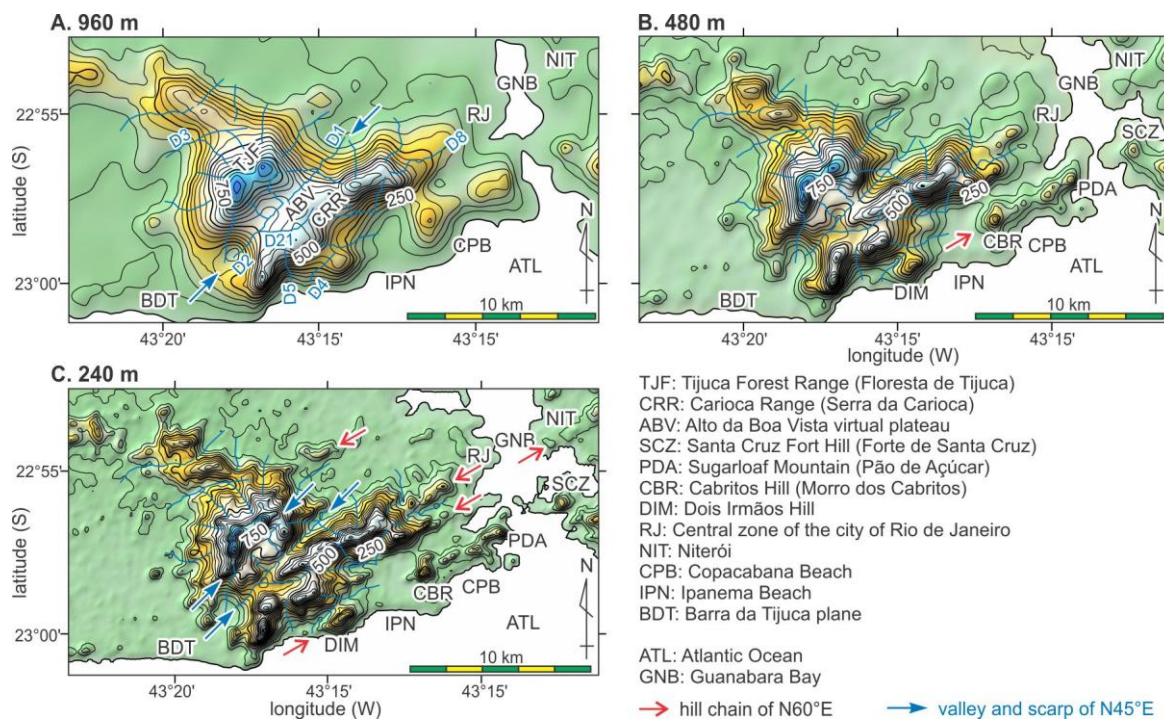


**Figure 3.** Summit level maps for the Tijuca massif and the adjacent areas based on ASTER GDEM of grid interval of: A) 960 m; B) 480 m; C) 240 m.

The map of 480 m of grid interval presents the valleys wider than 1 km showing more clearly the valleys of NE-SW direction. On this map, no drainage crosscuts the virtual ranges because main drainages of this massif are wider than 1 km and narrower than 2 km. This width is much wider than that of the felsic alkaline massifs (Motoki et al., 2008a; 2014). The virtual plateau is limited in Tijuca Forest side (Figure 3B). The small rocky hills of Santa Cruz Fort (SCZ), Sugarloaf Mountain (PDA), Cabritos Hill (CBR), and Dois Irmãos Hill (DIM), form a chain striking N60°E with length of 15 km.

The summit level surface of 240 m of grid interval presents the drainages wider than 500 m. Around the highest zone of the Tijuca Forest, the narrow and short drainages form a radial system. The virtual plateau is limited in a small area of 2.5 km (NE-SW) x 0.8 km (NW-

SE) with altitude of 500 to 550 m. The intrusion of Alto da Tijuca quartz diorite occurs at this site. On this map, the hill chain of N60°E is expressed more clearly. In addition, there are four more hill chains of the same direction (Figure 3C, red arrows). That is, the direction of Carioca Range and the hill chains is different from the orientation of wide valleys.

The base of the Tijuca massif seems to be alluvial coastal plane of sedimentary environment. However, in fact it is composed of small hills constituted by basement rocks. They have an altitude of 100 m and are in erosive environment, so-called half-orange (*meia laranja*). The summit level surface constituted by the top of the half-oranges represents a peneplane, called Rio de Janeiro Lowland (RJL, *Baixada Fluminense*, Aires et al., 2012).

## BASE LEVEL MAPS

In a massif of advanced erosive stage, base level map shows state of vertical erosion of drainages. It is useful to detect knickpoints related to vertical tectonic movements.

The base level map of 960 m of grid interval shows smooth surface. The star-shaped dendritic border is almost imperceptible. Only

of Alto da Boa Vista valley zone (ABV, Figure 4A) is expressed. The Tijuca Forest Range (TJF) has semi-circular form with a diameter of 6 km. Carioca Range (CRR) has elongated shape, striking N30°E, with an extension of 14 km (ENE-SWS) x 5 km (NWN-ESE).

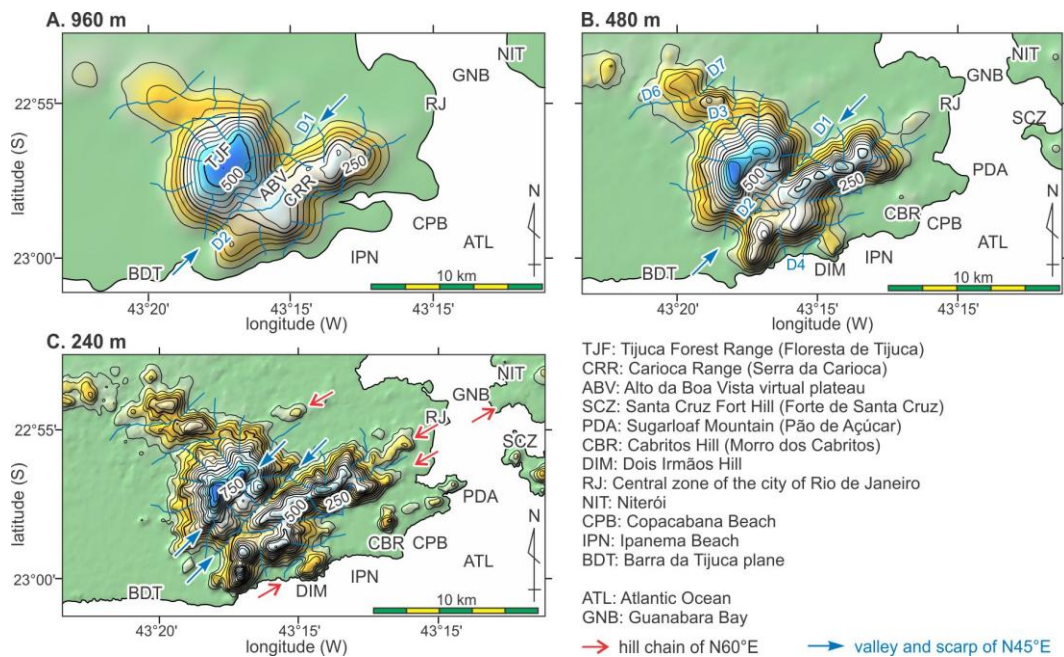


**Figure 4.** Base level maps for the Tijuca massif and the adjacent area based on ASTER GDEM of grid interval of: A) 960 m; B) 480 m; C) 240 m.

The map of 480 m of grid interval presents some valleys striking NE-SW, as D1, D2, D3, D4, D6, and D7. The radial drainages around the highest zone of the Tijuca Forest can be slightly observed. The dendritic shape of the massif border is not so expressive. Different from the alkaline massifs, no high-declivity marginal scarp is observed. The hill chain from Santa Cruz Fort (SCZ) to Dois Irmãos Hill (DIM) is not expressed on this map. With the

exception of the Dois Irmãos, they are equal to or smaller than 1 km.

The base level surface of 240 m of grid interval exhibits clearly all of the drainages wider than 500 m, including the radial system around the highest zone. The dendritic shape of the massif border and the hill chains of N60°E also are clearly observed. The half-oranges are little expressive because most of them are smaller than 0.5 km.

### RELIEF AMOUNT MAPS AND MCI

The relief amount map indicates average declivity of the unit cell of the grid. The relief amounts of the Tijuca massif have positive correlation to the altitude, that is, high relief amount zones are present in high altitude areas. There are high relief amount zone at Tijuca Forest Range (TIJ), Carioca Range

(CRR), Gávea Rock (GAV), and Usina (USN). The Usina is situated exceptionally at the bottom of Alto de Boa Vista valley zone along D1. This valley is delimited by subvertical walls exposing biotite gneiss and garnet biotite gneiss.

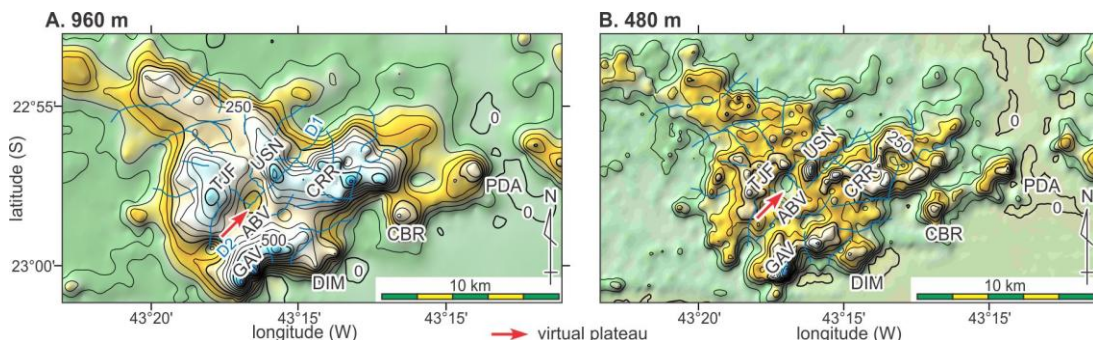


**Figure 5.** Relief amount maps for the Tijuca massif and the adjacent area based on ASTER GDEM of grid interval of: A) 960 m; B) 480 m. GAV - Gávea Rock; TJF - Tijuca Forest Range; USN - Usina valley; CRR - Carioca Range; PDA - Sugarloaf Mountain; CBR - Cabritos Hill; DIM - Dois Irmãos Hill.

In the high relief amount zones, large-scale landscapes can occur. Relief amount maps indicate the mean risk of the target unit cell area from prehistoric time up to the present. The cell size in discussion is 960 m (Figure 5A) or 480 m (Figure 5B). The relief amount value is not always related directly to the present-day debris-flow type landslide risk because most of the large landslide of Rio de Janeiro area took place in the prehistoric time. The landslides of historic heavy rainfall, such as of 1996 and 2007, formed the rock exposures of small size in comparison with the old ones present in Tijuca massif.

Different from the alkaline intrusive massifs, Tijuca massif has no ring-shaped high

relief amount zone. A low relief amount zone is at Alto da Tijuca Boa Vista (Figure 5, ABV, arrow) with an extension of 1 km (NE-SW) x 0.5 km (NW-SE). It corresponds to the central part of the virtual plateau on the summit level map of 960 m of grid interval (Figure 3A).

The MCI diagram for Tijuca massif exhibits a convex quadratic regression curve (Figure 6A). This curve is open in comparison with that of the alkaline intrusive massifs (Figure 6B). The macro concavity index (MCI) is -0.5 and it is significantly higher than those of the alkaline massifs. That is, Tijuca gneissic massif has relatively concave landform than the intrusive massifs of felsic alkaline rocks.

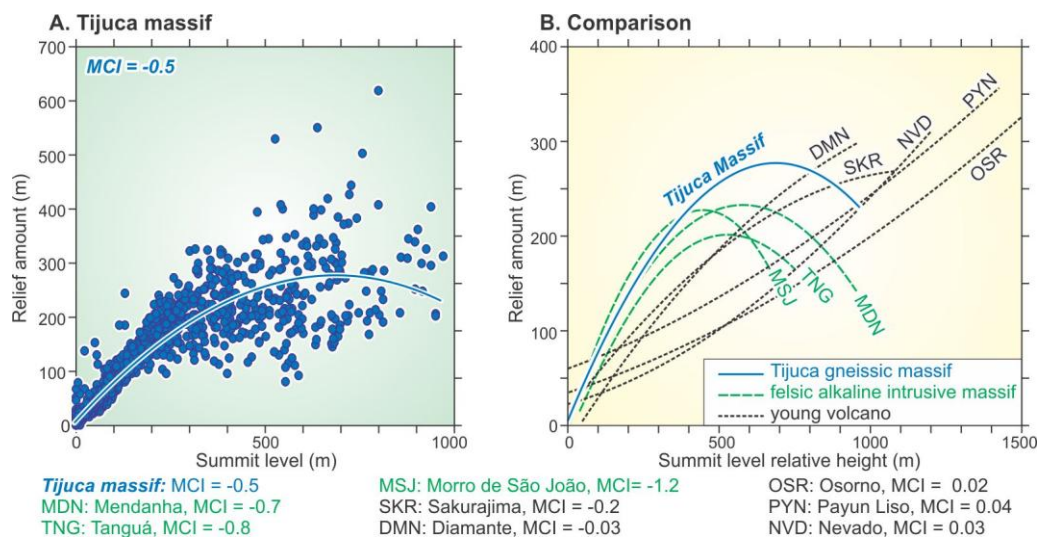


**Figure 6.** The MCI diagram for Tijuca massif based on the summit level and relief amount data of 480 m of grid interval (A) and its comparison with alkaline intrusive massifs and young volcanoes (B). The data of the other massifs are after Motoki et al. (2012a; 2014). MDN - Mendanha; MSJ - Morro de São João; TNG - Tanguá (felsic alkaline intrusions of the State of Rio de Janeiro, Brazil); SKR - Sakurajima volcano (Kyushu Island, Japan); DMN - Cerro de Diamante volcano, NVD - Nevado volcano; PYN - Payún Liso volcano (Mendoza, Argentina), OSR - Osorno volcano (Chile).

## ALTITUDE DISTRIBUTION HISTOGRAM

Hypsometric diagram is useful for regional geomorphologic interpretations, especially for detection of palaeo surfaces and active fault displacement. Tijuca gneissic massif shows Eiffel Tower-like near-exponential pattern. On the other hand, the felsic alkaline intrusive massifs present pyramid-like near-linear pattern (Figure 7A).

The difference becomes more expressive on the altitude distribution

histogram (Figure 7B), which corresponds to the differentiation function of hypsometric diagram. Tijuca massif shows an Eiffel Tower-like pattern and Morro de São João, a church bell-like one. The data of Morro de São João demonstrate the morphologic characteristics of nepheline syenite massifs, such as top swell (TS), virtual plateau (VP), and marginal scarp (MS).

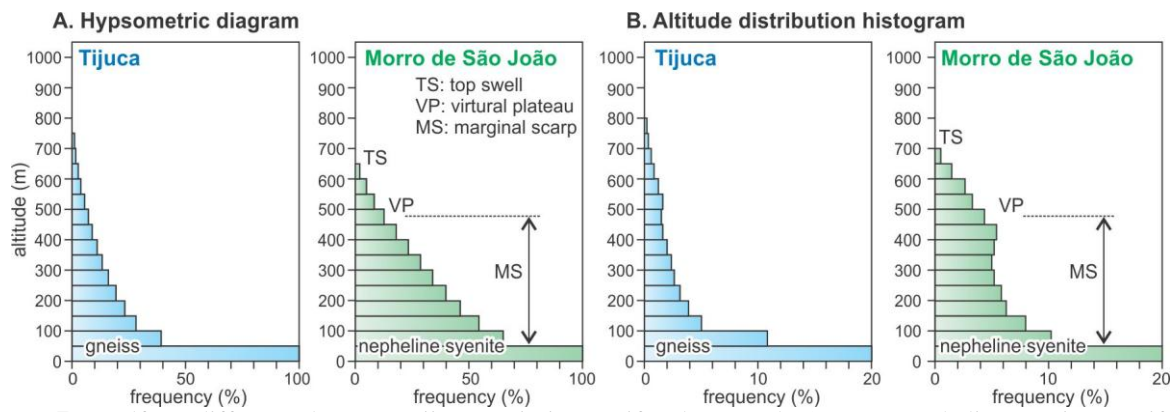


**Figure 7.** Landform difference between Tijuca gneissic massif and Morro de São João nepheline syenite massif: A) Hypsometric diagram; B) Altitude distribution histogram.

For the studies of erosive resistance of the base rock, the data of active erosion zone are useful and those of active sedimentation zone are useless. On the foot of the massif, there is an active sedimentation zone made up mainly of recent deposits of fan, landslide, debris, and constitute alluvial plane (Figure 8A). In the Rio de Janeiro Lowland, it occurs generally in the altitude lower than 50 m. The authors defined the threshold altitude which divides the sedimentary lowland and the erosive

highland using first-order differentiation of the altitude distribution histogram. In this article, the authors consider the low altitude active sedimentation zone to be the altitude with relative frequency higher than 10% on the first-order differentiation (Figure 8B). In most of the massifs of this region, the threshold altitude is 50 m, and in few cases, 100 m. The altitude range from the threshold to the mountain top is called effective data range.

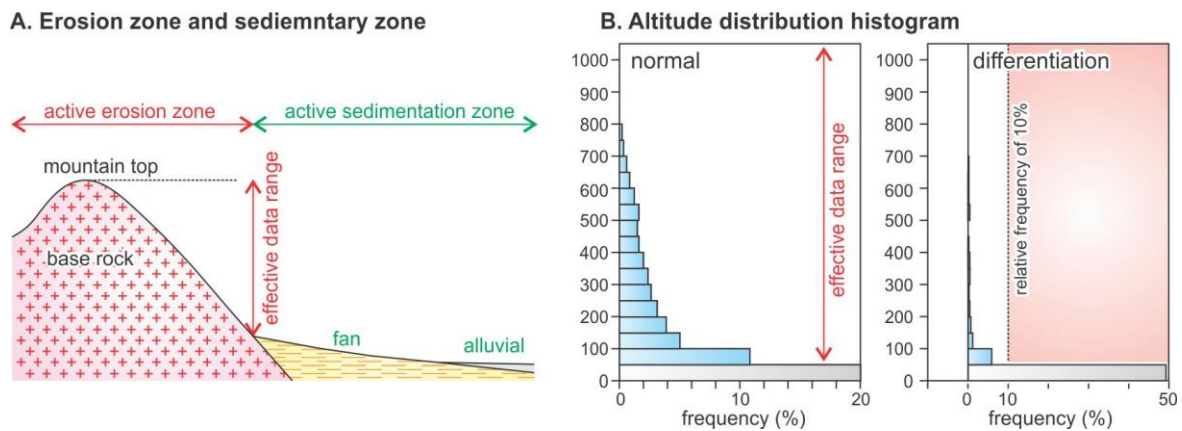


**Figure 8.** Definition of the effective altitude range for erosion data: A) Schematic illustration of morphologic characteristics for the active erosion and sedimentation zones; B) Threshold altitude using first-order differentiation diagram of the altitude distribution histogram.

The effective data of Tijuca massif show an Eiffel Tower-like pattern, with a slightly exceptional distribution of the highest area of Tijuca Forest (Figure 9A, arrow). On the other hand, those of the felsic alkaline massifs present a church bell-like pattern

(Figure 9). The difference is due to the absence of marginal scarp in Tijuca massif. The marginal scarp is attributed to high erosive resistance of nepheline syenite (Motoki et al., 2008a; 2014; 2015a).

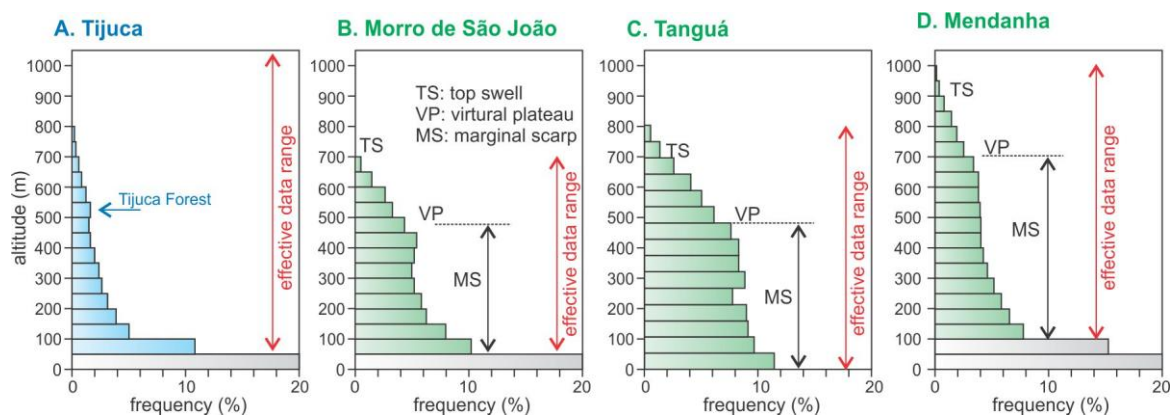


**Figure 9.** Altitude distribution histogram of Eiffel Tower-like pattern of Tijuca gneissic massif (A) and church bell-like pattern of felsic alkaline intrusive massifs of Morro de São João (B), Tanguá (C), and Mendanha (D).

### THREE-DIMENSIONAL CONCAVITY INDEX

Motoki et al. (2008a; 2012a; 2014) and Motoki K. et al. (2014) introduced macro concavity index (MCI) in order to express concavity of massif landform. Strongly negative MCI indicates convex landform, such as of the felsic alkaline intrusive massifs, and positive MCI, concave landform, as of young stratovolcanoes.

Motoki et al. (2015a) proposes another parameter which also represents the concavity of massif landform based on the effective data of altitude distribution histogram, called volume-normalised three-dimensional massif concavity index (TCI). This parameter

corresponds to three-dimensional extension of area-normalised stream concavity index (SCI; Demoulin, 1998; Zaprowski et al., 2005).

This parameter is calculated by the following equation:  $TCI = 1 - 2 \times V$ . The V is the sum of the normalised values of the effective data on the hypsometric diagram (Figure 10). The TCI ranges from -1 to 1. When  $TCI > 0$ , the massif has concave three-dimensional landform, and when  $TCI < 0$ , convex landform. The massifs with positive TCI are common and those with negative TCI are rare.

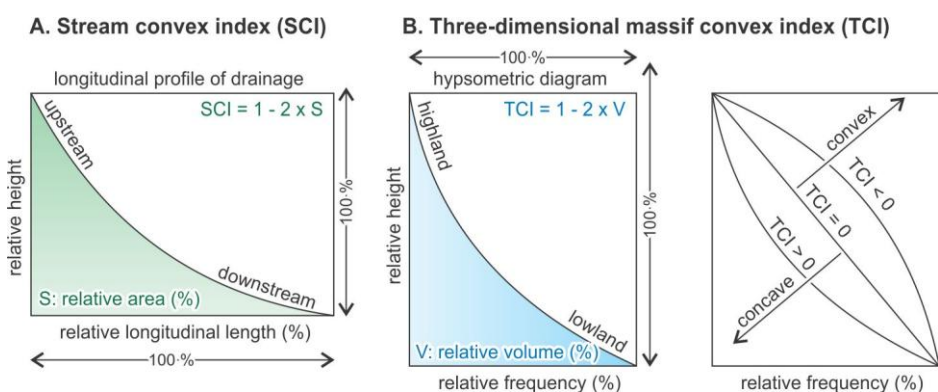


**Figure 10.** Principle of concave indexes (Motoki et al., 2015a; b): A) Area-normalised stream concave index (SCI; Demoulin, 1998; Zaprowski et al., 2005); B) Volume-normalised three-dimensional massif concave index (TCI), which is proposed in this article.

Tijuca massif has high TCI of 0.54. On the other hand, Tanguá and Morro de São João nepheline syenite massifs have low TCI, respectively of 0.16 and 0.20. Mendanha massif has MCI of 0.34, which is higher than the other alkaline massifs and lower than Tijuca gneissic

massif. In fact, this massif is constituted either by syenitic or gneissic rocks (Motoki et al., 2008a). The gneiss is exposed generally in the altitude lower than 300 m. The diagram of TCI vs. MCI distinguishes granitic and syenitic massifs (Figure 11).

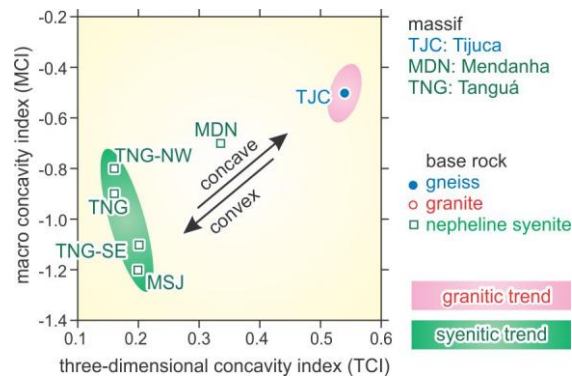


**Figure 11.** Diagram of volume-normalised three-dimensional concavity index (TCI) vs. macro concavity index (MCI). The data of the felsic alkaline massifs are after Motoki et al. (2008a; 2014; 2015a; b) and those of Pedra Branca granitic massif are unpublished data of the authors. TNG-NW and TNG-SE are respectively north-western and south-eastern areas of Tanguá massif.

## DISCUSSION

The previous studies tended to attribute erosive vulnerability of massifs to the mineral and chemical composition of the base rock. However, recent geomorphologic studies of the massifs of State of Rio de Janeiro, including Tijuca Massif, indicate that the controlling factors are not so simple.

Among the massifs standing on Rio de Janeiro Lowland, Mendanha (Motoki et al., 2008a), Tanguá (Motoki et al., 2015b), and Morro de São João (Motoki et al., 2014) have available geomorphologic studies with the help of summit level and base level techniques. They are felsic alkaline intrusive massifs and the morphologic relief is originated from differential erosion.

Tijuca massif also stands on the same peneplane with similar relative height but it is constituted by orthogneiss and paragneiss. Its morphologic characteristics are widely different from the alkaline intrusive massifs: 1) The drainages are wider and of gentler declivity; 2) Marginal scarp is absent; 3) Virtual plateau area is much smaller; 4) MCI and TCI are lower.

The highest area of Tijuca Forest Range exceptionally has landform slightly convex (Figure 9A, arrow) with radial drainage system (Figure 4B, C).

The concave landform is attributed to erosive vulnerability of the gneiss in comparison the nepheline syenite. The failure stress by uniaxial compression of gneissic rocks is generally lower than 90 MPa and that of the syenitic rocks is higher, about 170 MPa (Petrakis et al., 2010). In addition to the lower mechanical strength, banded gneiss texture helps surface water percolation along biotite concentration planes into deep sites of the rock body, which enables formation of thick regolith (Figure 12A). On the other hand, clay-rich impermeable regolith originated from the chemical weathering of nepheline syenite prevents surface water percolation into the rock body, preserving it without weathering (Figure 12B), the phenomenon called weathering passivity (Motoki et al., 2008a; Petrakis et al., 2010).

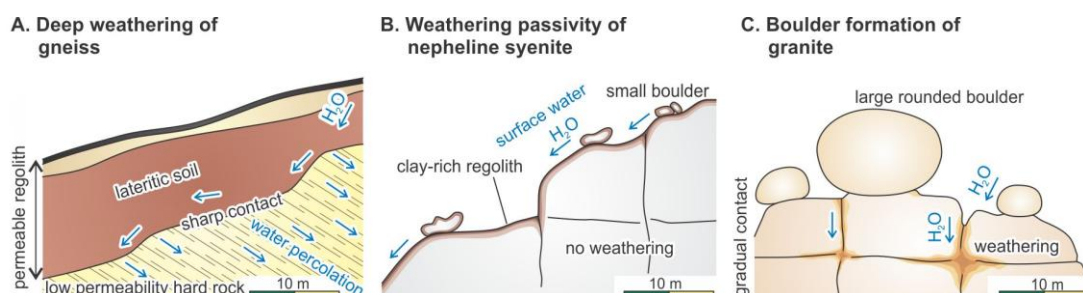


**Figure 12.** Weathering modes of different types of base rock under the humid tropical climate of Rio de Janeiro, modified from Petrakis et al. (2010): A) Deep weathering of gneiss and thick regolith formation by surface water percolation along the banded texture; B) Nepheline syenite covered by clay-rich impermeable regolith; C) In-situ large boulders of granite formed by surface water percolation along the cooling fractures.

The fieldworks in Tijuca massif have revealed that the regolith on gneiss is thick, up to 30 m, due to strong chemical weathering. The contact between the lateritic regolith and unweathered rock is sharp. The regolith contains no large boulders. The surface water infiltrates into the regolith along the porosity. In the strong rainstorms by cloudburst, a large amount of water is accumulated at the bottom zone of regolith because the unweathered rock is much less permeable. The water-rich layer has low mechanical sustainability and the overlain regolith layer can slip, causing a large debris-flow type landslide with complete removal of the regolith.

The landslide forms a gneissic exposure on the hill slope. When the rock exposure surface is of gentle declivity, lower than  $35^\circ$ , new soil cover and the consequent forest recovery occur in a period of 10 years. When the rock surface is steeper, from  $35^\circ$  to  $60^\circ$ , rainfalls wash out the new soil and forest recovery is difficult. The upper part of the hill tends to be dry and the lower part tends to be wet (Figure 13A). Therefore, the chemical weathering of gneiss by surface water percolation and the consequent thick regolith formation tend to occur on the foot of hill.

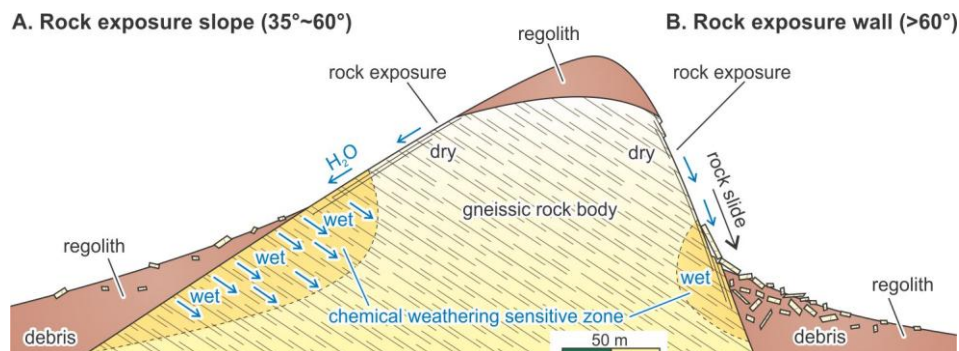


**Figure 13.** Schematic illustration of the evolution of large rock exposures of Rio de Janeiro area: A) Rock exposure slope ( $35^\circ\sim 60^\circ$ ) formed chemical weathering of gneiss and the consequent landslide at the foot of the slope: B) Wall of rock exposure ( $>60^\circ$ ) and rock-slide.

The successive landslides on the mountain foot make the rock exposure steeper and form of the hill becomes more convex. The walls of rock exposure with high declivity, more than  $60^\circ$ , are characterised by rock-slides (Figure 13B). The high peaks are covered by thin regolith and surrounded by high walls of gneiss exposure with convex surface (Figure

2A, B, D). The slightly convex landform (Figure 9A) with radial drainage system (Figure 4C) at the highest zone of the Tijuca Forest is attributed to this process. The proposed model provides a possible idea for the genesis for the large rock exposures of Rio de Janeiro, which constitute attractive landscape of the international sightseeing spots.

## CONCLUSION

The morphologic analyses of Tijuca gneissic massif with the help of summit level and base level technique, altitude distribution histogram, volume-normalised three-dimensional concave index (TCI), and macro concavity index (MCI) lead the authors to the following conclusions.

1. Tijuca massif has an extension of 15 x 10 km with a relative height of 1000 m. The summit level maps show absence of marginal scarp and limited area of virtual

plateau. The massif is divided into Tijuca Forest (NW) and Carioca Range (SE) by Alto da Boa Vista valley zone with strike of  $N45^\circ E$ . The Small rocky hills form five chains with  $N60^\circ E$  orientation. The orientations of large drainages and small rocky hills are discordant.

2. The base level maps show that the drainages wider than 1 km have orientation of  $N45^\circ E$ . The narrow and short drainages at the highest range zone form a radial system. Tijuca Forest Range, Carioca

Range, and Gávea Rock have high relief amount and are characterised by the walls of gneiss exposure, being the risk zones of large-scale landslide.

3. The effective data of the altitude distribution histogram for Tijuca massif show an Eiffel Tower-like pattern. The difference from a church-bell like pattern of the felsic alkaline intrusive massifs is due to the absence of high-declivity marginal scarp.
4. The volume-normalised three-dimensional concavity index (TCI) and macro

concavity index (MCI) for Tijuca massif are, respectively, 0.55 and -0.4, indicating a concave three-dimensional landform. These values are much larger than those of the Tanguá and Morro de São João felsic alkaline massifs, respectively, 0.16 to -0.9 and 0.20 to -1.2.

5. The concave landform of Tijuca gneissic massif is attributed to its erosive vulnerability in comparison with the nepheline syenite massifs because of lower uniaxial failure, gneiss texture, and minor effects of weathering passivity.

## ACKNOWLEDGEMENT

This article represents an extensional research of theme of the Master Degree of Samuel da Silva, one of the authors, which were performed at the Federal Fluminense University, Niterói, State of Rio de Janeiro,

Brazil. The authors are grateful to FAPERJ (scientific financial support foundation of the State of Rio de Janeiro) and PETROBRAS (Brazilian national petroleum company) for the financial supports.

## REFERENCE

1. AIRES, J.R.; MOTOKI, A.; MOTOKI, K.F.; MOTOKI, D.F.; RODRIGUES, J.G. Geomorphological analyses of the Teresópolis Plateau and Serra do Mar Cliff, State of Rio de Janeiro, Brazil with the help of summit level technique and ASTER GDEM, and its relation to the Cenozoic tectonism. **Anuário do Instituto de Geociências da Universidade Federal do Rio de Janeiro**, v. 35, n. 2, p. 105-123, 2012.
2. COELHO-NETTO, A.L.; AVELAR, A.S.; FERNANDES, M.C.; LACERDA, W.A. Landslide susceptibility in a mountainous geocosystem, Tijuca Massif, Rio de Janeiro: The role of morphometric subdivision of the terrain. **Geomorphology**, v. 87, n. 3, p. 120-131, 2007.
3. COELHO-NETTO, A.L.; AVELAR, A.S.; LACERDA, W.A. Landslides and Disasters in Southeastern and Southern Brazil. **Developments in Earth Surface Processes**, v. 13, p. 223-243, 2009.
4. DEMOULIN, A. Testing the tectonic significance of some parameters of longitudinal river profiles: the case of the Ardenne (Belgium, NW Europe), **Geomorphology**, n. 24, p. 189-208, 1998.
5. FERNANDES, N.F.; GUIMARÃES, N.F.; GOMES, R.A.T.; VIEIRA, B.C.; MONTGOMERY, D.R.; GREENBERG, H. Topographic controls of landslides in Rio de Janeiro: field evidence and modeling. **Geomorphic Impacts of Rapid Environmental Change**, v. 55, n. 2, p. 163-181, 2004.
6. GERALDES, M.C.; MOTOKI, A.; VARGAS, T.; IWANUCH, W.; BALMANT, A.; MOTOKI, K.F. Geology, petrography, and emplacement mode of the Morro dos Gatos alkaline intrusive rock body, State of Rio de Janeiro, Brazil. **Geociências**, Rio Claro, v. 32, n. 4, p. 625-639, 2013.
7. GUEDES, E.; HELIBRON, M.; VASCONCELOS, P.M.; VALERIANO, C.M.; ALMEIDA, J.C.H.; TEIXEIRA, W.; THOMÁZ FILHO, A. K-Ar and  $^{40}\text{Ar}/^{39}\text{Ar}$  ages of dykes emplaced in the on-shore basement of the Santos Basin, Resende area, SE. Brazil: implications for the south Atlantic opening and Tertiary reactivation. **Journal of South American Earth Sciences**, v. 18, p. 371-182, 2005
8. HEILBRON, M.; MACHADO, N. Timing of terrane accretion in the Neoproterozoic-Eopaleozoic Ribeira orogen (se Brazil). **Precambrian Research**, v. 125, p. 87-112, 2003.
9. HEILBRON, M.; MOHRIAK, W.; VALERIANO, C.M.; MILANI, E.; ALMEIDA, J.C.H., TUPINAMBÁ, M. From collision to extension: the roots of the southeastern continental margin of Brazil. In: Mohriak, W.U. and Talwani, M. (Eds.), **Geophysical Monograph**, American Geophysical Union, v. 115, p. 1-32, 2000.
10. HELMBOLD, R.; VALENÇA, J.G.; LEONARDOS JR., O.H.L. Mapa geológico do Estado da Guanabara, escala 1:50000, **Mapa Geológico**. Rio de Janeiro, DNPM, 1965.
11. KÜHN, A.; STÜWE, K.; TROUW, R.A. Metamorphic Evolution of the Ribeira Belt: Evidence from Outcrops in the Rio de Janeiro Area, Brazil. **Journal of Petrology**, v. 45, n. 11, p. 2303-2323, 2004.
12. MACHADO, N.; VALLADARES, C.; HEILBRON, M.; VALERIANO, C. U-Pb geochronology of the central Ribeira belt (Brazil) and implications for the evolution of the Brazilian Orogeny. **Precambrian Research**, v. 79, n. 3-4, p. 347-361, 1996.
13. MARQUES, E.G.A.; BARROSO, E.V.; MENEZES FILHO, A.P.; VARGAS JR., E.A.

- Weathering zones on metamorphic rocks from Rio de Janeiro - Physical, mineralogical and geomechanical characterization. **Engineering Geology**, v. 111, n. 1-4, p. 1-18, 2010.
14. MOTOKI, A.; ZUCCO, L.L.; SICHEL, S.E.; AIRES, J.R.; PETRAKIS, G.H. Desenvolvimento da técnica para especificação digital de cores e a nova nomenclatura para classificação de rochas ornamentais com base nas cores medidas. **Geociências**, Rio Claro, v. 25, n. 4, p. 403-415, 2006.
  15. MOTOKI, A.; SOARES, R.; NETTO, A.M.; SICHEL, S.E.; AIRES, J.R.; LOBATO, M. Genetic reconsideration of the Nova Iguaçu Volcano model, State of Rio de Janeiro, Brazil: eruptive origin or subvolcanic intrusion? **REM-Revista Escola de Minas**, Ouro Preto, v. 60, n. 4, p. 583-592, 2007. (a)
  16. MOTOKI, A.; SOARES, R.S.; LOBATO, M.; SICHEL, E.S.; AIRES, J.R. Weathering fabrics in felsic alkaline rocks of Nova Iguaçu, State of Rio de Janeiro, Brazil. **REM-Revista Escola de Minas**, Ouro Preto, v. 60, n. 3, p. 451-458, 2007. (b)
  17. MOTOKI, A.; SOARES, R.; NETTO, A.M.; SICHEL, S.E.; AIRES, J.R.; LOBATO, M. Geologic occurrence shape of pyroclastic rock dykes in the Dona Eugênia River Valley, Municipal Park of Nova Iguaçu, Rio de Janeiro. **Geociências**, Rio Claro, v. 26, n. 1, p. 67-82, 2007. (c)
  18. MOTOKI, A.; PETRAKIS, G.H.; SICHEL, S.E.; CARDOSO, C.E.; MELO, R.C.; SOARES, R.S.; MOTOKI, K.F. Landform origin of the Mendanha Syenitic Massif, State of Rio de Janeiro, Brazil, based on the geomorphological analyses by summit level map technique. **Geociências**, Rio Claro, v. 27, n. 1, p. 99-115, 2008. (a)
  19. MOTOKI, A.; SICHEL, S.E.; SOARES, R.S.; NEVES, J.L.P.; AIRES, J.R. Geological, lithological, and petrographical characteristics of the Itaúna Alkaline Intrusive Complex, São Gonçalo, State of Rio de Janeiro, Brazil, with special attention of its emplace mode. **Geociências**, Rio Claro, v. 27, n. 1, p. 33-44, 2008. (b)
  20. MOTOKI, A.; SICHEL, S.E.; SOARES, R.S.; AIRES, J.R.; SAVI, D.C.; PETRAKIS, G.H.; MOTOKI, K.F. Vent-filling pyroclastic rocks of the Mendanha, the Itaúna, and the Cabo Frio Island, State of Rio de Janeiro, Brazil, and their formation process based of the conduit implosion model. **Geociências**, Rio Claro, v. 27, n. 3, p. 451-467, 2008. (c)
  21. MOTOKI, A.; SICHEL, S.E.; PETRAKIS, G.H. Genesis of the tabular xenoliths along contact plane of the mafic dykes of cabo frio area, state of Rio de Janeiro, Brazil: Thermal delamination or hydraulic shear fracturing? **Geociências**, Rio Claro, v. 27, n. 2, p. 207-218, 2009.
  22. MOTOKI, A.; VARGAS, T.; IWANUCH, W.; SICHEL, S.E.; BALMANT, A.; AIRES, J.R. Tectonic breccia of the Cabo Frio area, State of Rio de Janeiro, Brazil, intruded by Early Cretaceous mafic dyke: Evidence of the Pan-African brittle tectonism ? **REM-Revista Escola de Minas**, Ouro Preto, v. 64, n.1, p. 25-36, 2011.
  23. MOTOKI, A.; VARGAS, T.; IWANUCH, W.; MELO, D.P.; SICHEL, S.E.; BALMANT, A.; AIRES, J.R.; MOTOKI, K.F. Fossil earthquake evidenced by the silicified tectonic breccia of the Cabo Frio area, State of Rio de Janeiro, Brazil, and its bearings on the genesis of stick-slip fault movement and the associated amagmatic hydrothermalism. **Anuário do Instituto de Geociências da Universidade Federal do Rio de Janeiro**, Rio de Janeiro, v. 35, n. 2, p. 124-139, 2012. (a)
  24. MOTOKI, A.; GERALDES, M.C.; IWANUCH, W.; VARGAS, T.; MOTOKI, K.F.; BALMANT, A.; RAMOS, M.N. The pyroclastic dyke and welded crystal tuff of the Morro dos Gatos alkaline intrusive complex, State of Rio de Janeiro, Brazil. **REM-Revista Escola de Minas**, Ouro Preto, v. 65, n. 1, p. 35-45, 2012. (b)
  25. MOTOKI, A.; SILVA, S.; SICHEL, S.E.; MOTOKI, K.F. Geomorphological analyses by summit level and base level maps based on the ASTER GDEM for Morro de São João felsic alkaline Massif, State of Rio de Janeiro, Brazil. **Geociências**, Rio Claro, v. 33, n. 1, p. 11-25, 2014.
  26. MOTOKI, A.; MOTOKI, K.F.; SICHEL, S.E.; SILVA, S.; AIRES, J.R. Principle and geomorphological applicability of summit level and base level technique using ASTER GDEM satellite-derived data and the original software Baz. **Acta Scientiarum Technology**, 2015 (a) (in press)
  27. MOTOKI, A.; SICHEL, S.E.; SILVA, S.; MOTOKI, K.F. Morphologic characteristics and erosive resistance of felsic alkaline intrusive massif of tanguá, State of Rio de Janeiro, Brazil, based on the ASTER GDEM. **Geociências**, 2015. (b) (in press).
  28. MOTOKI, K.F.; MOTOKI, A.; SICHEL, S.E. Gravimetric structure for the abyssal mantle exhumation massif of Saint Peter and Saint Paul Peridotite Ridge, Equatorial Atlantic Ocean, and its relation to the active uplift driving force. **Anais de Academia Brasileira de Ciências**, v. 86, n. 2, p. 395-412, 2014.
  29. PETRAKIS, G.H.; MOTOKI, A.; SICHEL, S.E.; ZUCCO, L.L.; AIRES, J.R.; MELLO S.L.M. Ore geology of special quality gravel and artificial sand: examples of alkaline syenite of Nova Iguaçu, State of Rio de Janeiro, and rhyolite of Nova Prata, State of Rio Grande do Sul, Brazil. **Geociências**, Rio Claro, v. 29, n. 1, p. 21-32, 2010.
  30. PIRES, F.M.; VALENÇA, J.G.; RIBEIRO, A. Multistage generation of granite in Rio de Janeiro, Brazil. **Anais da Academia Brasileira de Ciências**, v. 54, n. 3, p. 563-574, 1982.
  31. PENHA, H.M.; FERREIRA, A.L.; RIBEIRO, A.; AMADOR, E.S.; PENTAGNA, F.; JUNIOR, N.C.B.; BERNNER, T.L. **Projeto Carta Geológica do Estado do Rio de Janeiro, Folha Petrópolis**, Relatório final e mapa, Departamento de Recursos Minerais do Estado do Rio de Janeiro, Niterói, 1979.
  32. RAMLI, M.F.; YUSOF, N.; YUSOFF, M.K.; JUAHIR, H.; SHAFRI, H.Z. Lineament mapping and its application in landslide hazard assessment: a review. **Bulletin of Engineering Geology and the Environment**, v. 69, n. 2, p. 215-233, 2010.
  33. SICHEL, S.E., ESPERANÇA, S., MOTOKI, A., MAIA, M., HORAN, M.F., SZATMARI, P., ALVES, E.C., MELLO SLM. Geophysical and geochemical evidence for cold upper mantle beneath the Equatorial Atlantic Ocean. **Brazilian Journal of Geophysics**, v. 26, n. 1, p. 69-86, 2008.

34. STEWART, S.; TURNER, S.; KELLEY, S.; HAWKESWORTH, C.; KRISTEIN, L.; MANTOVANI, M. 3D -  $^{40}\text{Ar}/^{39}\text{Ar}$  geochronology in Paraná continental flood basalt province. **Earth Planet, Science Letters**. v. 143, p. 95-109, 1996.
35. VALERIANO, C.M.; TUPINAMBÁ, M.; SIMONETTI, A.; HEILBRON, M.; ALMEIDA, J.C.H.; EIRADO, L.G. U-Pb LA-MC-ICPMS geochronology of Cambro-Ordovician post-collisional granites of the Ribeira belt, southeast Brazil: Terminal Brasiliano magmatism in central Gondwana supercontinent. *Journal of South American Earth Sciences*, v. 32, n. 4, p. 416-428, 2011.
36. ZAPROWSKI, B.; PAZZAGLIA, F.; EVENSON, E. Climatic influences on profile concavity and river incision, **Journal of Geophysical Research**, electronic edition, v. 110, n. F3, doi:10.1029/2004JF000138, 2005.

*Manuscrito recebido em: 11 de Julho de 2014*  
*Revisado e Aceito em: 04 de Dezembro de 2014*